Energy 109 (2016) 803–817

Contents lists available at ScienceDirect

Energy

journal homepage: www.elsevier.com/locate/energy

Numerical investigation of the energy performance of a guideless irregular heat and mass exchanger with corrugated heat transfer surface for dew point cooling

Peng Xu [a, b], Xiaoli Ma [a], Thierno M.O. Diallo [a], Xudong Zhao [a, *], Kevin Fancey [a], Deying Li [b], Hongbing Chen [b]

[a] School of Engineering, University of Hull, HU6 7RX, UK
[b] Beijing University of Civil Engineering and Architecture, Beijing 100044, China

ARTICLE INFO

Article history:
Received 24 June 2015
Received in revised form
28 March 2016
Accepted 19 May 2016

Keywords:
Evaporative cooling
Dew point cooling
Heat and mass exchanger
Heat and mass transfer
Simulation
Energy performance

ABSTRACT

The paper presents an investigation into the energy performance of a novel irregular heat and mass exchanger for dew point cooling which, compared to the existing flat-plate heat exchangers, removed the use of the channel supporting guides and implemented the corrugated heat transfer surface, thus expecting to achieve the reduced air flow resistance, increased heat transfer area, and improved energy efficiency (i.e. Coefficient of Performance (COP)) of the air cooling process. CFD simulation was carried out to determine the flow resistance (K) factors of various elements within the dry and wet channels of the exchanger, while the 'finite-element' based 'Newton-iteration' numerical simulation was undertaken to investigate its cooling capacity, cooling effectiveness and COP at various geometrical and operational conditions. Compared to the existing flat-plate heat and mass exchangers with the same geometrical dimensions and operational conditions, the new irregular exchanger could achieve 32.9%–37% higher cooling capacity, dew-point and wet-bulb effectiveness, 29.7%–33.3% higher COP, and 55.8%–56.2% lower pressure drop. While undertaking dew point air cooling, the irregular heat and mass exchanger had the optimum air velocity of 1 m/s within the flow channels and working-to-intake air ratio of 0.3, which allowed the highest cooling capacity and COP to be achieved. In terms of the exchanger dimensions, the optimum height of the channel was 5 mm while its length was in the range 1–2 m. Overall, the proposed irregular heat and mass exchanger could lead to significant enhanced energy performance compared to the existing flat-plate dew point cooling heat exchanger of the same geometrical dimensions. To achieve the same amount cooling output, the irregular heat and mass exchanger had the reduced size and cost against the flat-plate ones.

1. Introduction

Conventional mechanical vapour compression air conditioning systems consume high power, create high carbon emission and cause severe environmental impact. Several alternative cooling systems, e.g. adsorption, absorption, desiccant and ejector cooling, are less efficient in terms of energy utilisation and practicality [1]. Evaporative cooling, by using water evaporation to absorb heat, is an extremely low energy and environmentally friendly cooling principle. However, owing to the theoretical constraint of the air wet-bulb temperature, this system has very limited temperature reduction potential which has restricted its wider application [2–5]. Dew point cooling, being a new form of Indirect Evaporative Cooling (IEC), can break up this limit, thereby achieving higher cooling efficiency than conventional IEC. This technology is established on a M-cycle heat and mass exchanger which basically has the cross- or counter-flow types [6–10].

Researches on the M-cycle cross- and counter-flow heat and mass exchangers for dew point evaporative cooling are numerous. These included the experiment-based, simulation-based and combined experiment and simulation works. In terms of the experiment, Bruno F. [8] constructed a flat-plate cross-flow heat and mass exchanger which used a special medium with high water retention and wickability characteristics as the wet channel, and a

* Corresponding author.
E-mail address: xudong.zhao@hull.ac.uk (X. Zhao).

http://dx.doi.org/10.1016/j.energy.2016.05.062

Nomenclature

a	side length of computational element, m
A	heat and mass transfer area of computational element, m^2
COP	Coefficient of Performance
C_P	specific heat capacity, kJ/kg °C
De	equivalent diameter, m
Dh	hydraulic diameter, m
en	latent heat, kJ/kg
g	gravity acceleration, m/s^2
h	convection coefficient, $W/(m^2\ °C)$
h_m	mass transfer coefficient, m/s
H	height, m
hum	humidity ratio, kg/kg
i	enthalpy, kJ/kg
l	length, m
l_0	thermal entry length, m
Le	Lewis number
Nu	Nusselt number
n	number
P	pressure, Pa
$\triangle P$	pressure drop, Pa
$\triangle Pf$	frictional pressure loss, Pa
$\triangle Plocal$	local pressure loss, Pa
$Qcooling$	cooling capacity, kW
Qm	mass flow rate, kg/s
Pr	Prandtl number
Re	Reynolds number
s	area, m^2
T	temperature, °C
Tf	air temperature, °C
u	air velocity, m/s
W	electric power, kW
x	distance, m

Subscripts

air	air
air, wet	wet air
dp	dew point
dry	dry channel
dry, in	inlet of dry channel
dry, out	outlet of dry channel
f	airflow
fan	fan
in	inlet
out	outlet
steam	water steam
pump	pump
vap	evaporated water
w	channel wall
water	water
wb	wet-bulb
wet	wet channel
wet,in	inlet of wet channel
wet, out	outlet of wet channel

Greek

λ	conduction coefficient, kW/m °C
α	thermal diffusivity, m^2/s
λf	coefficient of friction resistance
ζ	coefficient of local resistance
σ	surface wettability factor
$\triangle$	difference between two states
μ	dynamic viscosity, kg/(m s)
ρ	density, kg/m^3
φ	working air fraction over inlet air
ε	effectiveness
η	efficiency

moisture-impervious membrane as a dry channel. The tests indicated that the exchanger had a dew point effectiveness of 75%, which was relatively lower under the given operational condition. Coolerado (USA) developed a cross-flow heat exchanger with perforated holes on the flow paths. A test indicated that this type of exchanger could obtain the wet bulb and dew point effectivenesses of around 80% and 50% under the specified operational condition [11], which is around 20% higher than that of the conventional IEC heat exchangers. Velasco G. at al [12] carried out an experiment study into a polycarbonate-made IEC heat exchanger. The results indicated the IEC heat exchanger could obtain higher cooling capacity and also increased cooling effectiveness when spraying water against the cooling air. Higher outdoor air temperature or air flow rate helped obtain enhanced cooling performance of the system. Riangvilaikul et al. [13] carried out an experimental investigation into a novel dew point evaporative cooling system, indicating that the wet-bulb and dew point effectivenesses were in the range 92%–114% and 58%–84%, under the pre-set operational condition.

In terms of the computer simulation and combined modelling and experiment, J. Lin et al. [10] presented a numerical study of a dew point evaporative cooling system with counter-flow configuration. The study found the saturation point of working air occurring at a fixed point regardless of the inlet air conditions, minimum intensity point of water evaporation of 0.2–0.3 m from the entrance and overall heat transfer coefficient above 100 $w/(m^2\ K)$ in wet channel of the unit. Tuisidasani et al. [14] studied the relation between the Coefficient of Performance and air velocity for a tube type IEC heat and mass exchanger using both modelling and experimental methods, indicating that the maximum COP of the IEC unit was 22 at the primary air velocity of 3.5 m/s and the secondary air velocity of 3 m/s, leading to 10.4 °C of primary air temperature drop. Riangvilaikul and Kumar [15] presented a numerical study of a counter-flow heat exchanger, which involved the numerical simulation of the heat and mass transfer processes within the flow channels, and experimental validation [13]. Reasonable agreement was achieved between the numerical and experimental results, giving 5–10% of deviation in terms of the outlet air temperature and effectiveness, respectively. The dew point effectiveness of the unit was in the range 58%–84%, higher than cross-flow exchanger. Zhao et al. [16] conducted a numerical study into a novel counter-flow flat-plate heat and mass exchanger for dew point cooling, indicating that cooling effectiveness and energy efficiency of the exchanger were largely dependent on the dimensions of the air flow passages, air velocity and working-to-intake air ratio, and less dependent on the temperature of the feed water. Zhan et al. [6] carried out a comparative study into the M-cycle counter-flow and cross-flow flat-plate heat exchangers for indirect evaporative coolers (IEC), indicating that the counter-flow exchanger offered greater (around 20% higher) cooling capacity,

greater (15%–23% higher) dew-point and wet-bulb effectiveness, and lower (10% lower) COP. Further, Zhan et al. [17] also conducted a numerical study into a cross-flow dew point cooling heat exchanger, indicating that the average air velocities in dry and wet channels should be less than 1.77 m/s and 0.7 m/s respectively, the optimum working-to-product air ratio was 50%, the channel's length-to-height ratio should be in the range 100–300, while its height should be in the range 4 mm–6 mm. Cui et al. [18] presented a computational fluid dynamics (CFD) study into the counter-flow heat and mass exchanger, in order to analyse the impacts of operational conditions and geometrical parameters on the cooler's performance. The discrepancy regarding to temperature distributions and outlet air conditions provided by the model was found to be within ±10%. The simulation results indicated that the cooling effectiveness of the exchanger was increased with lower air velocity, smaller channel height, larger channel length-to-height ratio, and higher working-to-intake air flow ratio. Cui et al. [19] developed a modified log mean temperature difference (LMTD) method for predicting thermal performance of the present M-cycle counter-flow and cross-flow heat and mass exchanger. The results were found to be within ±8% discrepancy when compared to experimental data.

The extensive literature reviews undertaken by the authors indicated that previous researhces on IEC heat and mass exchangers were mostly focused on the flat-plate types. This type of exchanger was found to still have limited temperature reduction potential when undertaking the dew point cooling, resulting in problems of larger size and higher cost which have impeded its broader application. The research methods applied to this kind of research were either by experiment, computer simulation and combined modelling and experiment. In terms of the computer simulation, traidtioanl 'finite-element' or 'finite-differenital' approaches were the basic principles that were used to carry out the 'differential' treatment to the tradtional energy and mass transfer and fluid flow equations, thus formulating the special numerical computational programs. Owing to the non-conventional geometries/materials incorporated in the computational channels, e.g., irregular channel supporting guides, bulk of the perforated holes, and variable inlet and outlet geometries, as well as different roughness conditions of the smooth (aluminum) and rough (fibre) heat transfer surfaces, which have unknown resistance factors, simulation on pressure drop and COP were largely based on the assumptions that have caused the significant discerepancies compared to the real measument data.

To tackle the above identified problems, the research proposed a novel irregular heat and mass exchanger which, compared to conventional flat-plate heat and mass exchangers, removed the use of the channel supporting guides and implemented the corrugated heat transfer surface. This is expected to increase the heat and mass transfer area between the dry and wet channel air streams, thus increasing the heat transfer rate of the exchanger. Further, this is also expected to decrease the flow resistance of the air when travelling across the dry and wet channels. As a result, the new exchanger is expected to achieve significantly higher energy efficiency (COP), cooling effectiveness, as well as cooling capacity, thus leading to a high efficient and low cost cooling solution. To improve the simulation accuracy and credibility, both CFD and finite-element based Newton-iteration numerical simulations will be applied. The logic is to use CFD simulation to predict the flow resistance (K) factors of the elements within both the dry and wet channels, and then introduce these factor values into the 'finite-element' based Newton-iteration numerical model to investiage the energy performance of the irregular heat and mass exchanger for various dimensions and operating conditions, thus recommending the optimum geometrical dimension and operational condition. Simultaneously, the numerical model will also be applied to simulate the energy performance of the traditonal flat-plate heat and mass exchanger under the same geometrical dimensions and operational condition as to the irregular heat ans mass exchanger. The results for the both exchangers will be compared in order to justify the performance enhancement level of the new exchanger relative to the existing one. In line with these initiative efforts, the research will help develop an innovative heat and mass exchanger with enhanced cooling and energy performance, which in turn will lead to the reduced cost and size of the cooler at the same cooling output and make it competitive to the conventional mechanical vapour compression air conditioners.

2. Configuration of the irregular heat and mass exchanger and relevant computational channel/elements for simulation

Schematic of the irregular heat and mass exchanger is shown in Fig. 1. For each exchanging plate, its inlet and outlet portions are made into the flat geometry for the convenience of air and water distribution within the exchanger's channel space; while its main portion is made into the corrugated geometry for increasing the heat and mass transfer area between the two parts of air. Compared to the traditional flat-plate heat and mass exchanger which has the triangular supporting guides between the two parallel plates (see Fig. 2), the new exchanger will be able to achieve a higher heat transfer rate owing to the increased heat transfer area. It, meanwhile, will also be able to achieve a lower flow resistance owing to elimination of the triangular channel supporting guides. As a result, energy performance of the dew point air cooler with the irregular exchanger, represented by the system's COP, would be significantly improved.

When constructing a dew point heat exchanger, whether flat-plate or irregular ones, wet surfaces of the two adjacent plates are against each other to build a wet channel. Similarly, the dry surfaces of two adjacent plates are against each other to build a dry channel. A dry channel is always adjacent to one or more wet channels. Fig. 3(a) and Fig. 3(b) show the flow channels for the irregular and flat-plate exchangers. The cross-sectional area of each irregular channel, either dry or wet, is two-times that of the trianglar channel in the flat-plate exchanger, while the triangular channel is enclosed by the heat exchanging plate and the channel supporting guides.

Considering the heat transfer between a dry channel and its neighborhood wet channels, the computational channels are established for both the flat-plate and irregular heat and mass exchanger structures, as shown schematically in Fig. 4(a) and (b). The equal-sized cross-sectional area is the base for parallel comparison of the both. Furthermore, two comparable computational elements, with both dry and wet channels, are identified and selected. Comparison between the two elements indicated that a corrugated element has much larger (2 times) heat transfer area.

It is also noticed that the irregular channel has FOUR side-walls whilst the flat-plate channel has SIX side-walls including the channel-supporting guides, indicating that the flat-plate channel will create a higher resistance to the passing air, leading to the increased flow resistance. The geometry-related pressure drops at the both channels will be simulated using CFD in order to determine the relevant air flow resistance factors, pressure drop and energy consumption of the fans.

Operational procedures of both the irregular and flat-plate heat and mass exchangers for dew point cooling are same. The intake (mostly ambient) air firstly enters the dry channels through the side-wall intalled flat trapzoid end, as shown in Figs. 1 and 2; the air then travels across the dry channels whereby it loses heat to the adjacent wet channels, thus leading to certain temperature drop. At

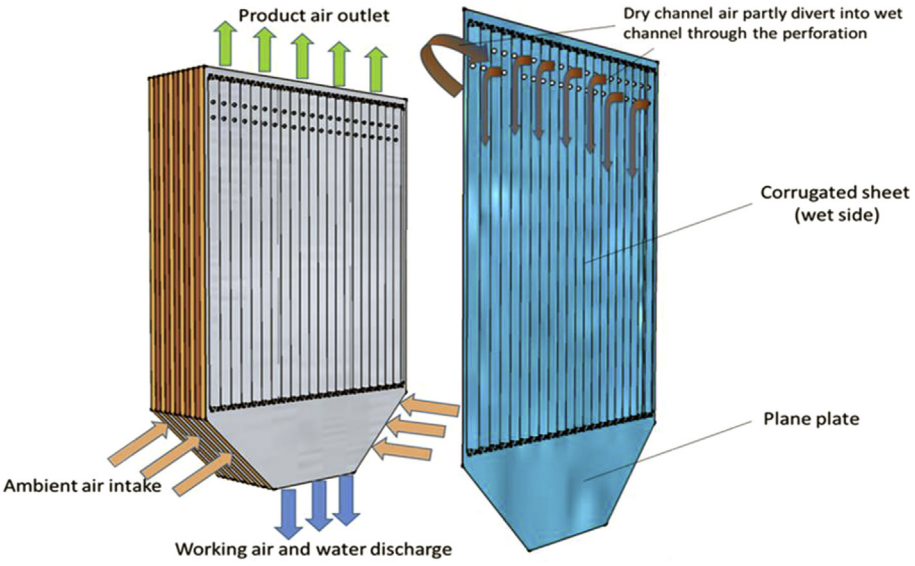

Fig. 1. Schematic drawing of the irregular heat and mass exchanger with corrugated heat transfer surface.

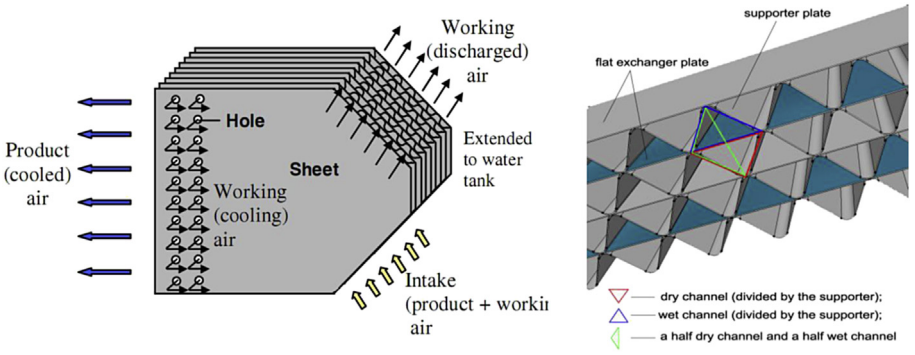

Fig. 2. Schematic of the flat-plate heat exchanger stacks.

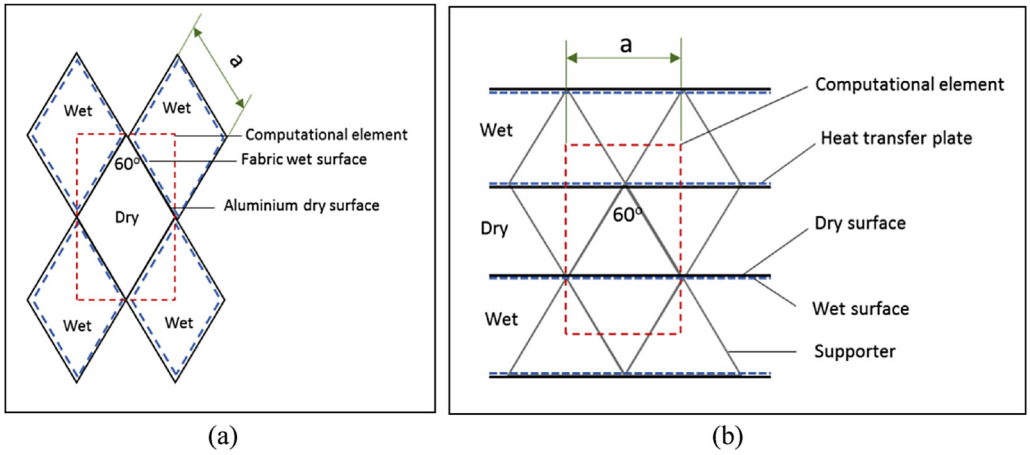

Fig. 3. Cross section view (a) irregular exchanger (b) flat plate exchanger.

the end of the dry channels, the air is splitted into two parts: one, called product air, is delivered into the conditioned space to perform cooling; while the remaining part, called working air, is diverted into the adjacent wet channels to help evaporating. Within the wet channels, the working air flows backwards, absorbing the heat transferred from the dry channels and receiving the moisture evaporated from the surface of the wet channels, thus completing a heat and mositure transition process from one part air to another, which leads to the generation of the chilled product air.

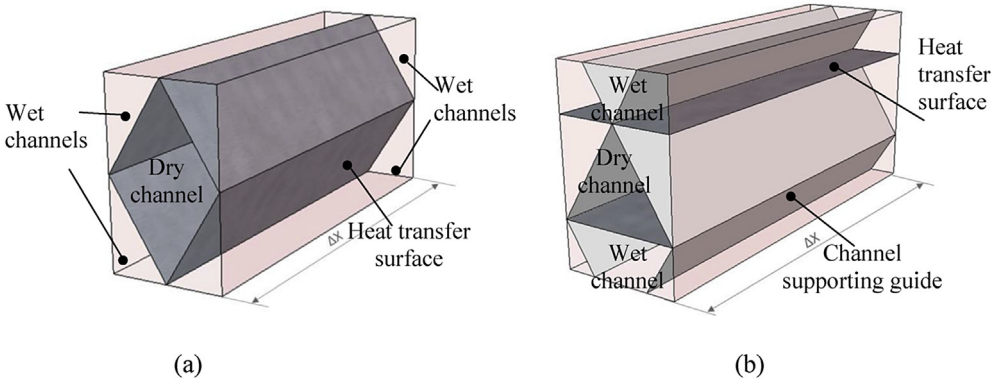

Fig. 4. Computational elements (a) irregular exchanger (b) flat plate exchanger.

3. Simulation method and theoretical equations

3.1. Simulation set-up and related assumptions

The computational elements for the both types of exchangers, which contain a dry channel and part of its adjacent wet channels (refer to Figs. 2 and 3), have the equal-sized cross-sectional area and thus, are considered as the base for simulation and comparison. 'Finite element' approach will be applied to make 'differential' treatment to the traditional energy and mass equilibrium equations, thus establishing the relevant differential equations based on each element. Within a single element, Newton iteration method will be applied to peruse the equilibrium state in terms of heat and mass transfer. To simplify the simulation process and mathematical analysis, the following assumptions have been made:

(1) For the irregular and flat-plate structures, the heat exchanging sheets and channel supporting guides were considered as the element's boundary surfaces.
(2) The heat and mass transfer process within the exchanger was considered to be adiabatic, i.e, no heat transfer occurring between the exchanger body and the surroundings.
(3) The heat and mass transfer process within the elements was assumed to be at steady state.
(4) The heat transfer via the channel walls was in the vertical direction. The convective heat transfer was considered as the dominant mechanism for the heat transfer between the airflow and water film/channel walls. The channel walls were impervious to water moisture.
(5) The wet channel surfaces were equally saturated with the water film, which was assumed to have the same temperature as to the channel wall surface.
(6) The thermal resistance of the channel wall was assumed to be negligible, indicating that there was no temperature difference between the dry and wet sides of the wall.
(7) Air was assumed to be an incompressible gas; air velocity was considered to be uniform within a single computational channel.

Along the channel length, each computational channel was divided into numerous computational elements. The typical geometrical set-up of the computational element and the whole modular exchanger are listed in Table 1, where the surface roughness of the wet channel material, i.e., fabric, is quoted from Ref. [20].

3.2. Mathematical equations for heat and mass transfer

For the computational element, the energy and mass equilibrium differential equations are shown as follows:

(1) Energy balance within a dry element

The air enthalpy difference between the inlet and outlet of a dry element is equal to the amount of heat transferred between the airflow and channel walls.

$$\Delta i_{dry} = C_P \cdot Qm_{dry} \cdot \Delta Tf_{dry} = h_{dry} \cdot \left(Tf_{dry} - T_w\right) \cdot \Delta A \tag{1}$$

(2) Mass balance in a wet element

The moisture content difference between the inlet and outlet of a wet element is equal to the amount of water evaporated across the wet surface.

$$\Delta hum_{wet} = h_m \cdot \rho_{air,wet} \cdot \left(hum_w - hum_{air,\,wet}\right) \cdot \sigma \cdot \Delta A \tag{2}$$

Where, hum_{wall} and hum_{wet} are the humidity ratio of the working air at the wet channel wall temperature and wet channel air temperature respectively. The difference between hum_{wall} and hum_{wet} is the inherent driving force for water evaporation occurring on the wet channel surface. σ is the wettability of the surface material, which is defined as the ratio of the wetted surface area to the total surface area. σ is affected by the water diffusivity of surface material.

The convective mass transfer coefficient between the working air flow and wet channel surface is expressed as a function of the convective heat transfer coefficient and the Lewis number, as follow [21]:

$$\frac{h}{h_m} = \rho \cdot Cp \cdot Le^{1-n} \tag{3}$$

where by n = 1/3.

The convective heat transfer coefficient between the air flow and the channel wall along the flow path is a variable, which is mainly determined by the flow regime. Under the low airflow velocity and small channel size (i.e. $Re < 2300$) condition, the air flows within both the dry and wet channels are laminar [21]. The thermal entry length for the laminar airflow in the dry/wet channels can be expressed as the function of the relevant Reynolds numbers and Prandtl numbers, as follow [22]:

$$l_0 = 0.05 \cdot De \cdot Re \cdot Pr \tag{4}$$

For the entrance region ($x \le l_0$), the Nusselt number can be

Table 1
Basic pre-setting parameters for simulation.

Parameters	Value
Channel length (m)	1.0
Cross-sectional side length of the irregular channel – a* value (m)	0.01
Element number per channel	500
Irregular sheet dimension: L × W × h (m)	1.0 × 0.5 × 0.00866
Exchanger module dimension: L × W × H (m)	1.0 × 0.5 × 0.433
Surface wettability factor	1.0
Fabric surface roughness (μm)	23.83
Aluminum sheet surface roughness (μm)	1
Working air ratio	0.5
Velocity of inlet air (m/s)	1.0

calculated using the following empirical correlation [21]:

$$Nu = 1.86\left(\frac{Re\cdot Pr}{\frac{x}{De}}\right)^{\frac{1}{3}}\cdot\left(\frac{\mu_f}{\mu_w}\right)^{0.14} \quad (5)$$

While in the fully developed region ($l_0 \le x \le l$), the Nusselt number is constant [22]:

$$Nu = 2.47 \quad (6)$$

According to the definition of Nusselt number, the convective heat transfer coefficient could be expressed as follow:

$$h = \frac{Nu\cdot\lambda}{De} = 1.86\left(\frac{Re\cdot Pr}{\frac{x}{De}}\right)^{\frac{1}{3}}\cdot\left(\frac{\mu_f}{\mu_w}\right)^{0.14}\cdot\frac{\lambda}{De} \quad (7)$$

(3) Energy balance of the airflow in the wet element

The air enthalpy difference between the inlet and outlet of a wet element is equal to the sum of the heat transferred from the dry to wet elements and the change of air flow enthalpy in the wet element owing to evaporation, which leads to change in humidity ratio of the air.

$$\Delta i_{wet} = C_P\cdot Qm_{wet}\cdot\varphi\cdot\Delta Tf_{wet} = \Delta Q_{wet} + \Delta i_{steam} \quad (8)$$

where,

$$\Delta Q_{wet} = h_{wet}\cdot(T_w - Tf_{wet})\cdot\Delta A \quad (9)$$

$$\Delta i_{steam} = h_m\cdot\rho_{air,wet}\cdot(hum_w - hum_{wet})\cdot Cp_{steam}\cdot Tf_{wet,out}\cdot\sigma\cdot\Delta A \quad (10)$$

(4) Conservation of water mass between the inlet and outlet of a wet element

The variation of the water flow rate between the inlet and outlet of the computational wet element is equal to the amount of water evaporated from the element surface.

$$\Delta Qm_{water} = h_m\cdot\rho_{air,wet}\cdot(hum_{wall} - hum_{wet})\cdot\sigma\cdot\Delta A \quad (11)$$

(5) Energy balance in a coupled dry & wet elements and variation of the air's humidity ratio

Water enthalpy difference between the inlet and outlet of a wet element is caused by heat transfer between the water and airflow in the dry/wet channels as well as the latent heat of the evaporated water.

$$\Delta i_{water} = \Delta Q_{dry} - \Delta Q_{wet} - \Delta Q_{vap} \quad (12)$$

$$\Delta i_{water} = \left(Qm_{water,out}\cdot Tw_{out} - Qm_{water,in}\cdot Tw_{in}\right)\cdot C_{Pwater} \quad (13)$$

$$\Delta Q_{vap} = h_m\cdot\rho_{air,wet}\cdot(hum_{wall} - hum_{wet})\cdot en_{steam}\cdot\sigma\cdot\Delta A \quad (14)$$

The latent heat of the evaporated water can be expressed as [21].

$$en_{steam} = 2446 + 1.86T_{water} \quad (15)$$

3.3. Methodology for evaluation of the performance of a dew point cooler

The following criteria are used to evaluate the performance of an IEC system: i) cooling capacity; ii) energy efficiency, i.e., Coefficient of Performance (COP); iii) wet-bulb effectiveness; and iv) dew-point effectiveness.

3.3.1. Cooling capacity

According to the formula provided by the ASHRAE Standard [23], the cooling capacity can be written as:

$$Q_{cooling} = Cp\cdot\left(Tf_{dry,in} - Tf_{dry,out}\right)\cdot(1-\varphi)\cdot Qm_{dry,in} \quad (16)$$

3.3.2. Coefficient of Performance

Coefficient of Performance (COP) [23] is expressed as the ratio of the cooling capacity ($Q_{cooling}$) to the total power consumption (W) of the cooler system:

$$COP = \frac{Q_{cooling}}{W_{fan} + W_{pump}} \quad (17)$$

Although actual power consumptions of the fan and pump are affected by numerous operational factors, the following theoretical formulas are often used to estimate their power needs.

The power consumption of a fan can be expressed as follow:

$$W_{fan} = \frac{\Delta P\cdot u\cdot s}{\eta_{fan}} \quad (18)$$

where, ΔP is the pressure drop of the airflow in the dry or (and) wet channels, which includes the frictional pressure loss along the channel, pressure loss from local fittings.

$$\Delta P = \Delta P_f + \Delta P_{local} \quad (19)$$

The frictional and local-fittings resistances of air flow can be calculated using the following equations [24]

$$\Delta P_{local} = \zeta \cdot \frac{\rho u^2}{2} \tag{20}$$

$$\Delta P_f = \lambda_f \cdot \frac{l}{Dh} \cdot \frac{\rho u^2}{2} \tag{21}$$

$$\Delta P = \left(\zeta + \lambda_f \frac{l}{Dh}\right) \cdot \frac{\rho u^2}{2} = K \cdot \frac{\rho u^2}{2} \tag{22}$$

The power consumption of a pump was calculated based on the water circulation rate and water raising height, by using the following equation:

$$W_{pump} = \frac{Qm_{water} \cdot \Delta P_{water}}{\rho_{water} \cdot \eta_{pump}} \tag{23}$$

The efficiencies of both the fan and pump were assumed to be 75%, and a factor of 1.8 for any unpredicted power loss was used in the simulation.

3.3.3. Determination of the flow channels' K values by CFD simulation

Owing to the complexity of the channel geometries in both the irregular and flat-plat heat and mass exchangers, it is difficult to sort out the local resistance factor ζ and frictional factor λ_f of each element included in the dry and wet channels. In this case, CFD tool was applied to aid this determination. This simulation was undertaken on the basis of laminar flow model by using ANSYS FLUENT 16.1, whereas the pressure-velocity coupling equations were solved by using SIMPLE algorithm. The numerical schemes for pressure and momentum were standard and first order upwind.

The flow domain was considered as three-dimensional. The boundary conditions are depicted in Fig. 5(a) and (b) and also illustrated below:

a) A symmetry conditions were imposed on external walls
b) "Inlet velocity" boundary was used at the dry air entrance.
c) "Outflow" condition was used for the dry air outlet and the wet air outlet. Wet side flow rate weighting was assumed as 0.3.
d) The surface roughness values of the wet and dry channels were those for fibre and aluminum, as shown in Table 1.
e) Geometry variations of the irregular channel at the inlet and outlet, i.e. from-flat-to-corrugated and from-corrugated-to-flat, were taken into consideration, while the air diverting from dry to wet channel via the perforated holes was also considered.

Table 2 provides a summary of K values, which were calculated using the CFD simulation results. For both the dry and wet channels, the irregular exchanger had smaller resistance factors than the flat-plat exchanger: the former was 55% of the latter. Fig. 6 shows the velocity and skin frictional coefficient contours at z = 0.5 m section.

3.3.4. Wet-bulb effectiveness

Wet-bulb effectiveness [25,26] is defined as the ratio of the difference between the inlet and outlet product air temperatures to the difference between the inlet-air's dry-bulb and wet-bulb temperatures, which is expressed as:

$$\varepsilon_{wb} = \frac{Tf_{dry,in} - Tf_{dry,out}}{Tf_{dry,in} - Tf_{dry,in\_wb}} \tag{24}$$

3.3.5. Dew-point effectiveness

Dew-point evaporating cooling systems can provide the product air with a temperature close to the dew point of the intake air; as such, the dew-point effectiveness [25,26] is defined as

$$\varepsilon_{dp} = \frac{Tf_{dry,in} - Tf_{dry,out}}{Tf_{dry,in} - Tf_{dry,in\_dp}} \tag{25}$$

4. Computer model set-up and validation

To enable simulation of the heat and mass transfer processes occurring in different channels/elements, a dedicated computational algorithm was developed to solve the above equations using the finite element and Newton-iteration method, which was operated under the EES (Engineering Equation Solver) basis [27]. The Newton-iteration algorithm [28] used for developing the

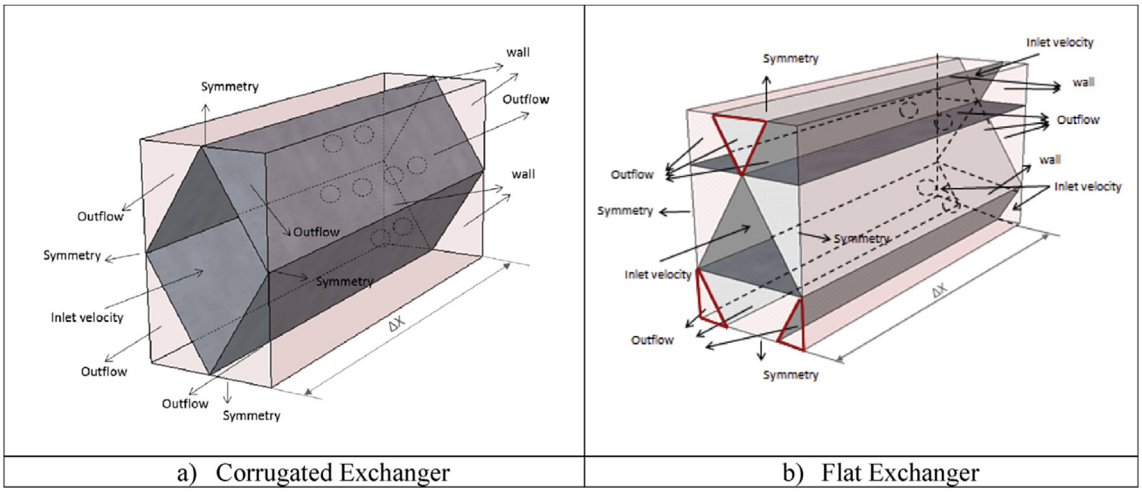

a) Corrugated Exchanger b) Flat Exchanger

Fig. 5. Flow domain and boundary conditions.

Table 2
Summary of the K values for both the irregular and flat-plate heat and mass exchanger.

Side	Mean velocity um (m/s)	Irregular exchanger		Flat plate exchanger	
		Flow resistance factor, K	Presure drop (Pa)	Flow resistance factor, K	Presure drop (Pa)
Dry	0.45	166.16	20.6	354.74	44
Wet	0.15	246.72	3.4	449.88	6.2
Dry	0.95	87.44	48.34	207.14	100.5
Wet	0.3	197	10.86	362.82	20
Dry	1.45	61.3	78.94	141.54	158
Wet	0.45	140.78	17.46	258	32
Dry	1.95	47.48	110.6	110.86	220
Wet	0.65	98.54	25.5	208.62	46
Dry	2.45	39.38	144.76	92.24	286
Wet	0.75	93	32.04	174.14	60
Dry	2.95	33.4	178	64.34	350
Wet	0.9	80.62	40	149.16	74

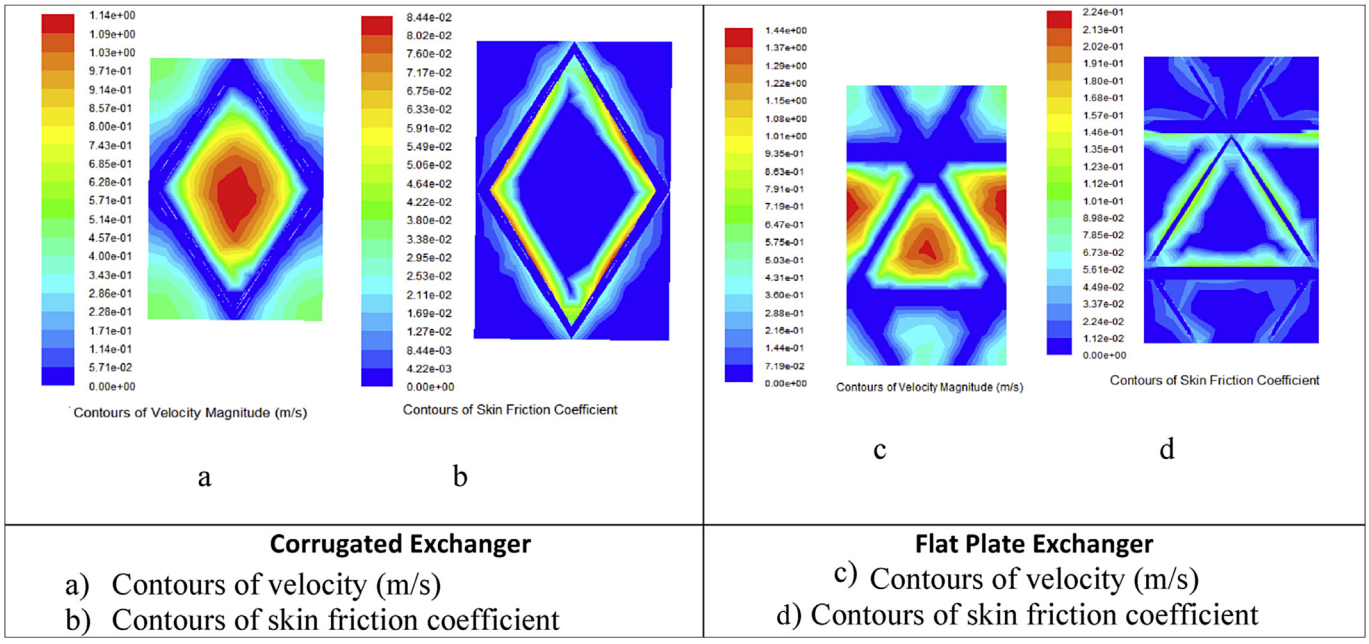

Fig. 6. Contours of velocities and skin friction coefficient at channel length of 0.5 m.

computer model is detailed as follows:

(a) Entering the geometrical and operational parameters relating to the dry/wet channels, including the channel length/height, number of computational elements, ratio of the working-to-intake air flow rate, water temperature and intake air condition, e.g. the dry-bulb temperature, wet-bulb temperature and velocity at the channel entrance.
(b) Assuming the start-up temperature for the intake dry air and dry channel wall, and determining the thermal-physical properties of dry air, i.e., density, specific heat capacity, thermal conductivity, dynamic viscosity and Prandtl number.
- Calculating the Reynolds number and determining the Nusselt number and convective heat transfer coefficient by using Eqs. (4)–(7).
- Calculating temperature of the air at the dry element outlet by using Eq. (1), and determining the temperature of the air at the dry channel outlet.
- Running the model by iteration until the required error allowance for the dry channel air temperature appeared.

(c) Assuming a start-up temperature for the outlet wet air and wet channel wall, and determining the thermal-physical properties of the wet air, i.e., density, specific heat capacity, thermal conductivity, dynamic viscosity and Prandtl number.
- Calculating the Reynolds number and determining the Nusselt number and the convective mass transfer coefficient by using Eqs. (3)–(7).
- Calculating the humidity ratio increment across the element by using Eq. (2), and determining the humidity ratio of the air at the outlet of the wet channel.

(d) Calculating the temperature of the air at the outlet of the wet channel by using Eqs. (8)–(10).
- Running the model by iteration until the required error allowance for the wet channel air temperature appeared.

(e) Calculating the water flow rate by using Eq. (11).
(f) Calculating the wall temperature based on the energy balance for the coupled dry & wet elements, by using Eqs. (12)–(15).
- Comparing the computed wall temperature with the previously assumed value, and

- Running the model by iteration until the required error allowance appeared.

(g) Completion of the model iteration process with reasonably accurate results.
(h) Calculating the cooling capacity, COP, and wet-bulb and dew-point effectiveness by using Eqs. (16)–(25).
(i) Delivering the simulation results and terminating the simulation process.

The computer model can be used for simulation of both the irregular heat exchanger and existing flat plate heat exchanger; the latter is treated as a specific geometrical set-up in the model, i.e., the zero height of the corrugated geometry. To validate the computer model, a simulation was carried out based on a flat-plate heat exchanger module which had the published experimental results [6,13]. These testing data were used to examine the effectiveness and accuracy of the model.

Given the channel height, length and width of 5 mm, 1200 mm and 80 mm respectively, intake air velocity of 2.4 m/s and working-to-intake air ratio of 0.33, which were the experimental conditions applied in ref. 13, simulation was carried out to generate a series of modelling results. These results were then compared with the testing data to examine the effectiveness and accuracy of the model, as shown in Fig. 7 [6,13]. It is found that the difference between the tested and simulated product air temperatures was in the range 0.1 °C–0.9 °C for various inlet air conditions; while the highest deviation occurred at the humidity ratio of 6.9 g/kg, giving an error rate of 4.9%. The difference between the tested and simulated cooling capacities was in the range 0.1–0.5 W under the referred testing conditions [13]; whilst the highest deviation occurred at the same humidity ratio condition, with an error rate of 5%. This comparison indicated that the accuracy of the computer model is around 5%.

Simulation was also conducted under different operational conditions presented in ref. 13, i.e., inlet air velocity of 0.83 m/s, working air ratio of 0.4 and inlet air conditions given in Table 3. The results were compared with the published experimental data, giving the derivation profile shown in Fig. 8. The difference between the modelling and published results was around 3.1% in average, indicating that the model could achieve a reasonable accuracy in predicting cooling performance of the dew point cooling heat exchanger.

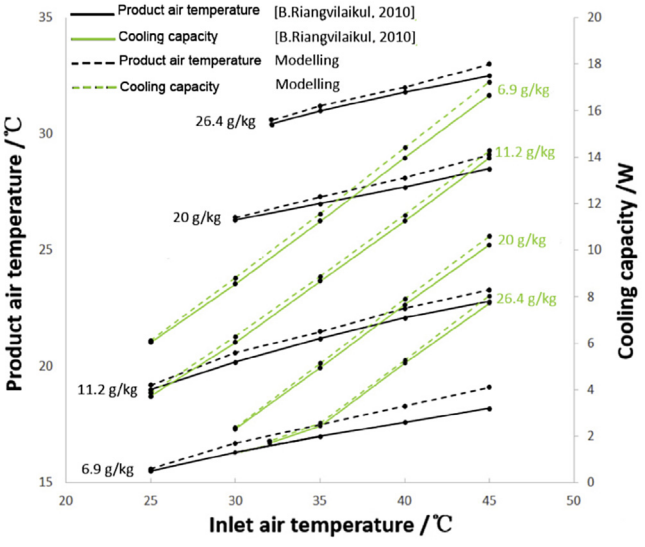

Fig. 7. Experimental validation – product air temperature and cooling capacity.

5. Comparative study of the performance of the novel irregular heat and mass exchangers and existing flat-plate heat exchanger

As previously addressed, the model developed in this study can be used to simulate the performance of both the irregular and flat-plate heat and mass exchangers. In this section, the performance of the two different heat and mass exchangers was investigated and compared under various inlet air conditions including temperature, humidity ratio, velocity, channel dimensions, and operational parameters including the working-to-intake air ratio and water temperature.

The simulation conditions applied to the comparative study were listed in Table 4, where the UK's typical cooling design temperatures were used. The inlet air condition and geometrical parameters of the heat and mass exchanger are the key factors impacting the performance of evaporating cooling. The simulation results are presented as follows:

5.1. Impact of the intake air parameters

5.1.1. Impact of the intake air temperature

Keeping the intake air humidity ratio at 0.015 kg/kg that is the typical London summer design parameter, impact of the intake air temperature on the performance of both the novel irregular and existing flat-plate heat and mass exchangers was investigated and the difference between the two exchangers was analysed; the results are shown in Fig. 9(a) and (b) respectively. For the both exchangers, increasing the intake air temperature led to significant increase in the cooler's cooling capacity and COP, which varied linearly with the temperature. However, the wet-bulb effectiveness, dew point effectiveness and product air temperature remained almost the same, with the figures of around 120%, 80% and 19 °C respectively.

Under the same operational condition, the irregular exchanger showed better performance than the flat-plate one. Although the indicative performance parameters, i.e., COP, cooling capacity and wet-bulb and dew point effectiveness of the two exchangers, had the similar variation trend versus the outdoor air temperature, the average COP and cooling capacity of the irregular exchanger were 31.4% and 34.2% higher than that of flat-plate one. The average wet-bulb and dew point effectiveness of the irregular exchanger were 122.1% and 82.2% respectively, which were 35% and 34.9% higher than that of the flat-plate one.

Compared to the flat-plate heat and mass exchanger, the irregular type was able to deliver higher cooling capacity and lower product air temperature. The cooling capacity and COP of the both exchangers increased linearly with the intake air temperature, owing to the fact that the increased air temperature could lead to the reduced air humidity ratio [25]. As a result, the evaporation rate and cooling capacity of the exchangers were eventually increased.

5.1.2. Impact of the intake air humidity ratio

Keeping the intake air temperature at 28 °C which is the typical London summer design temperature, impact of the humidity ratio on the performance of both the irregular and flat-plate heat and mass exchangers was investigated and the difference between the both was analysed. The results are shown in Fig. 10(a) and (b) respectively.

It is seen from the Fig. 10(a) and (b) that the indicative performance parameters, i.e., COP, cooling capacity and wet-bulb and dew point effectiveness, for the both exchangers showed similar trend of variation versus the humidity ratio. The cooling capacities and COPs for the both exchangers decreased quickly with the increase of humidity ratio of the intake air, indicating that the exchangers

Table 3
Climate conditions used in comparative simulation research.

No.	City	County	Dry bulb temperature (°C)	Wet-bulb temperature (°C)	Dew point temperature (°C)	Relative humidity
1	London	UK	28	20	16.0	48.2%
2	San Pablo	Spain	39.9	25.1	19.2	30.3%
3	Lisbon	Portugal	32.1	19.7	12.9	31.0%
4	Catania	Italy	34.1	21.6	15.5	32.9%
5	Athens	Greece	33.8	20.8	14.1	30.5%
6	Izmir	Turkey	35.5	20.4	12.1	24.4%
7	Copenhagen	Demark	24	17.3	13.4	51.5%
8	Helsinki	Finland	26.7	19.1	15.1	48.9%

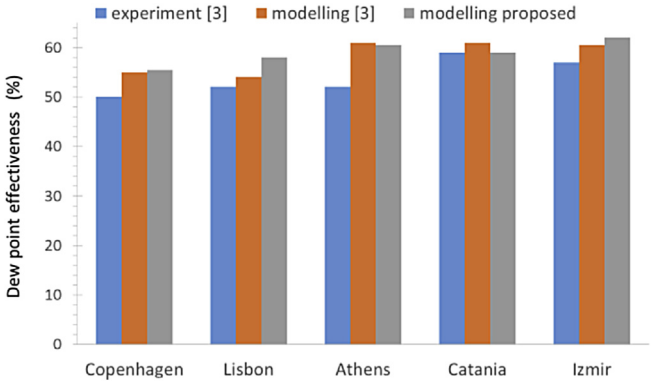

Fig. 8. Comparison of experimental and simulation results.

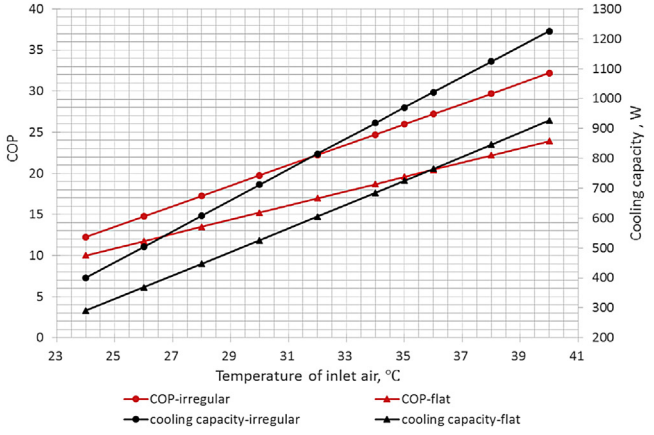

(a) Cooling capacity and COP

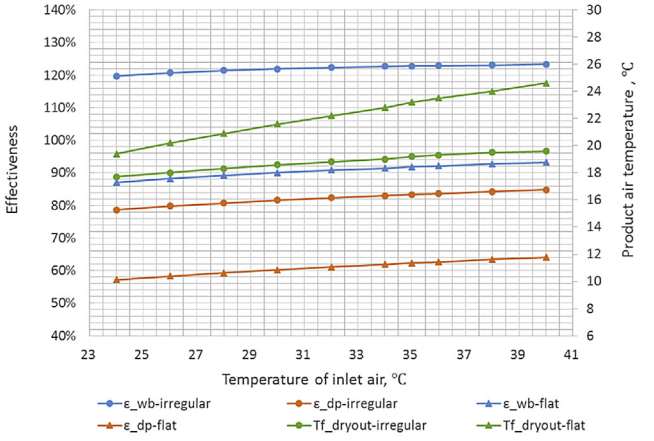

(b) Effectiveness and product air temperature

Fig. 9. Variation of performance with inlet air temperature (with constant moisture content).

may present better performance in a cool season owing to the reduced humidity ratio of the intake air. Meanwhile, both the wet-bulb and dew point effectivenesses decreased with the increase of humidity ratio. At a lower humidity ratio, e.g., 0.005 kg/kg, the irregular exchanger could obtain a temperature drop of 16 °C, while at a higher humidity ratio, e.g., 0.02 kg/kg, the temperature drop within the irregular module was only 3 °C.

Compared to the flat-plate exchanger, the irregular type could achieve a significantly enhanced performance. Under the pre-justified operational condition, the irregular type had 33.3% higher average COP and 37% higher average cooling capacity; while its average wet-bulb and dew point effectiveness were 35.5% and 35.3% higher than that of flat-plate type respectively. Under the low humidity ratio condition, the irregular version could achieve even higher cooling capacity than that under the high humidity ratio condition.

5.1.3. *Impact of the intake air velocity*

The intake air velocity is a factor impacting the flow rate and flow state of the air within the channels: the former affects the cooling capacity directly and the latter affects the heat and mass transfer rate which consequently impacts the cooling capacity of the cooler. Impact of the intake air velocity on the performance of both the irregular and flat-plate heat and mass exchangers was investigated and the difference between them was analysed. The results are shown in Fig. 11(a) and (b) respectively.

Cooling capacity of the both exchangers increased with the increase of air velocity, while the irregular type increased faster than that of the flat-plate one. When the air velocity varied from 0.3 m/s

Table 4
Pre-set operational conditions for simulation.

Channel length (m)	**Channel height (m)**	**Channel numbers**	**Element numbers per channel**	**Working-to-intake air ratio**	**Inlet water temperature (°C)**
1.0	0.01	2500	500	0.5	20
Dry bulb temperature of inlet air (°C)	**Wet-bulb temperature of inlet air (°C)**	**Inlet air velocity(m/s)**	**Surface wettability factor**	**Fan efficiency**	**Pump efficiency**
28	20	1.0	1.0	75%	75%

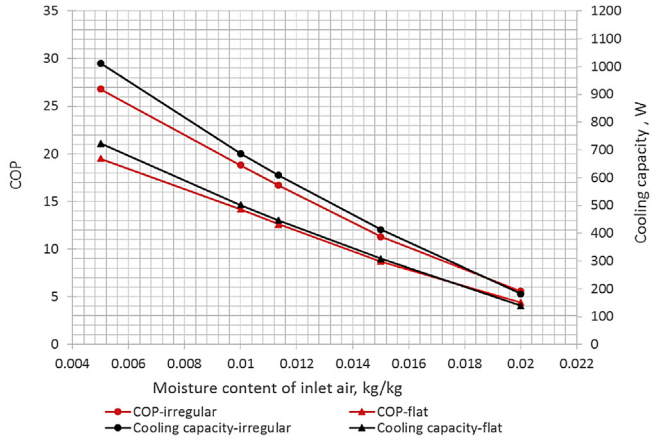

(a) Cooling capacity and COP

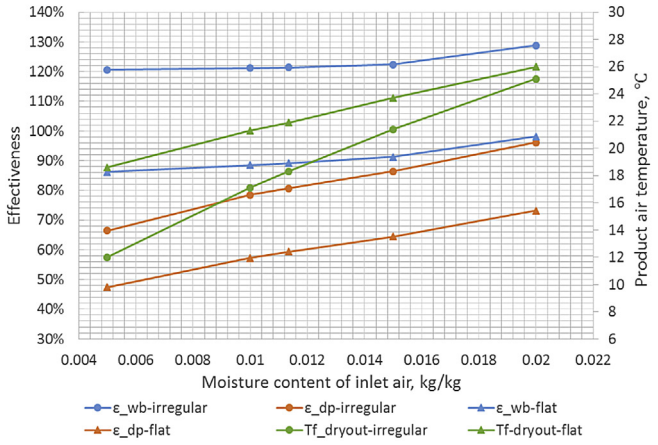

(b) Effectiveness and product air temperature

Fig. 10. Variation of the performance with inlet air humidity ratio.

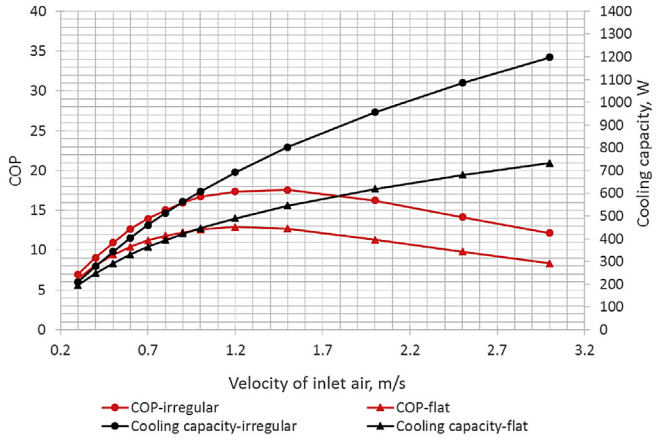

(a) Cooling capacity and COP

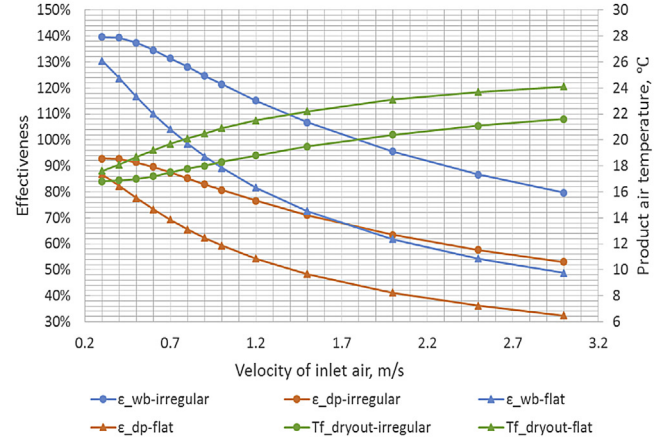

(b) Effectiveness and product air temperature

Fig. 11. Performance with the velocity of inlet air.

to 3.0 m/s, the cooling capacity of the irregular exchanger varied from 210 W to 1198 W, which were 35% and 63% higher than that of flat-plate type respectively.

For the both exchangers, COPs quickly increased with the increase of air velocity from 0.3 m/s to 1 m/s. When the velocity was greater than 1 m/s and below 1.5 m/s, COPs of the both exchangers reached their highest record and remained almost constant. When the velocity exceeded 1.5 m/s, COPs of the both exchangers started to fall. This phenomenon could be explained as follow: increasing the velocity led to the increase in the cooling capacity and increase in the pressure drop of the air flows. Since the COP is the ratio of the cooling output to the electrical power consumption, which is pressure drop relevant, an optimum velocity would be in existence enabling achieving the maximum COP. In this simulation process, 1 m/s–1.5 m/s would be the appropriate velocity range for the cooler design. As a lower air velocity, which led to a lower channel pressure drop and therefore lower power consumption of a fan, could produce a higher effectiveness, the velocity of around 1 m/s was considered the optimum choice for the both irregular and flat-plate exchangers. Under this condition, the COP and cooling capacity of the irregular exchanger were 16.7 and 608.2 W respectively, which were 33% and 36.2% higher than that of the flat-plate type.

For the both exchangers, the wet-bulb and dew point effectiveness decreased with the increase of air velocity. The wet-bulb and dew point effectiveness of the irregular type were 140% and 93% respectively when the air velocity was 0.5 m/s. These values actually fell to 121.4% and 80.7% respectively when the velocity increased to 1 m/s. Compared to the flat-plate exchanger, the irregular type has around 30% higher effectiveness in both the dew point and wet-bulb effectivenesses.

5.2. Impact of the channel dimensions

5.2.1. Impact of the channel height

The dimensions of a single channel, i.e., channel height and length, affect both the flow pattern and flow rate, which in turn influence the heat and mass transfer rate and cooling capacity of the heat and mass exchangers. Based on the exchanger stack of 1 m (height) × 0.5 m (width) × 0.433 m (thickness), impact of the channel height on the performance of the both exchangers was investigated and the difference in performance between the two exchangers was analysed. The results are shown in Fig. 12(a)–(d).

For a single channel, COP and cooling capacity increased with the channel height, while the pressure drop showed an opposite trend of variation. However, as the increase in channel height can lead to the reduced channel number of the heat exchanger, the overall cooling capacity of the heat exchanger would be reduced. Based on a fixed channel number, Fig. 12 (a) showed that the cooling capacities and COPs increased with the channel height.

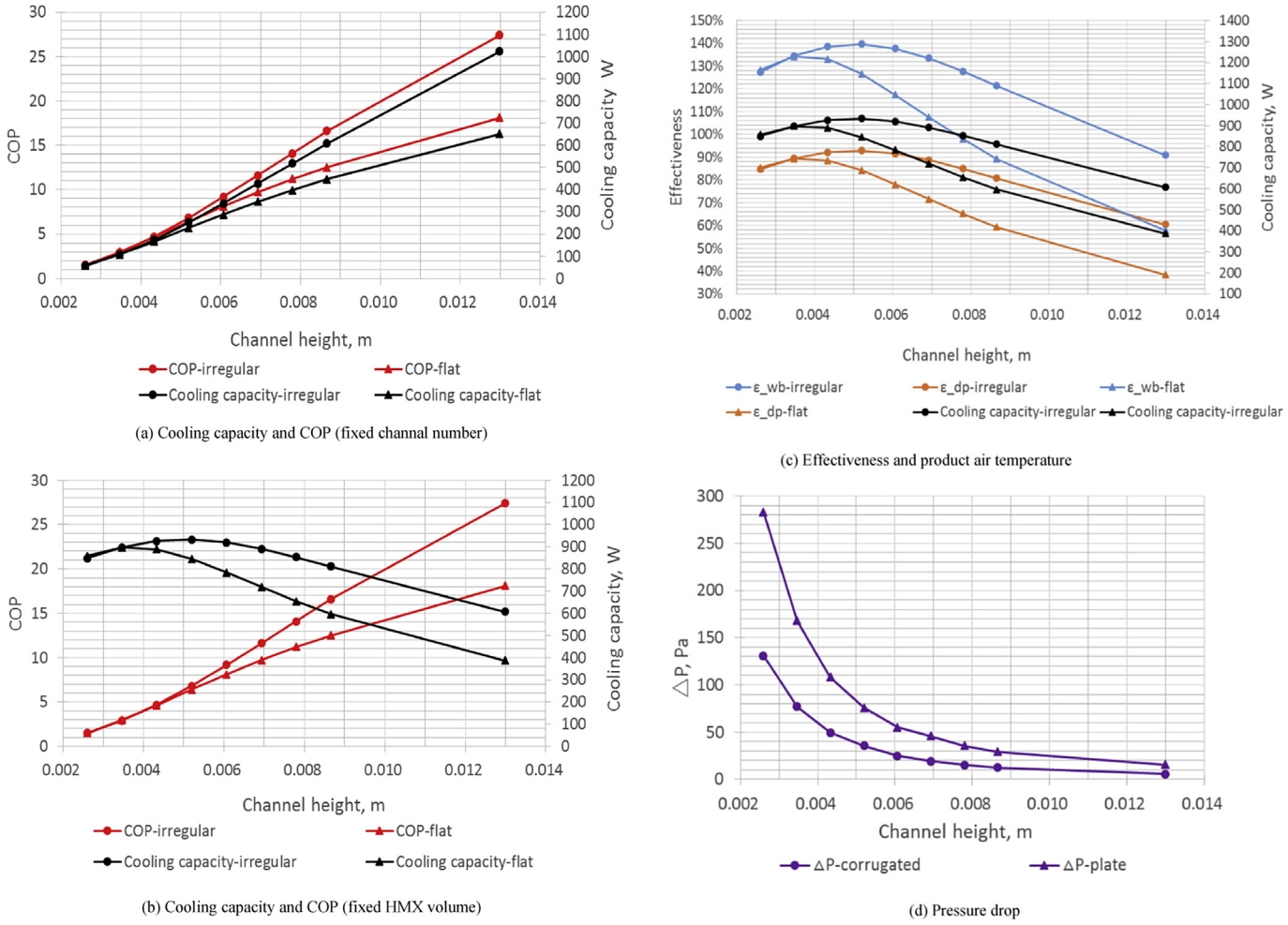

(a) Cooling capacity and COP (fixed channal number)

(b) Cooling capacity and COP (fixed HMX volume)

(c) Effectiveness and product air temperature

(d) Pressure drop

Fig. 12. Variation of performance with the channel height.

Based on the fixed exchanger dimensions, Fig. 12 (b) showed that the cooling capacity fell when the channel height was larger than 0.005 m.

Fig. 12(c) indicates that the optimum channel height for both the irregular and flat-plate exchangers was 0.005 m, at which the wet-bulb and dew point effectiveness of the both exchangers reached the maximum, i.e., 140.7%/129% and 93%/84% (irregular/flat-plate). As a result, the air temperature fell to the lowest, i.e., 16.8 °C for the irregular type and 16.5 °C for the flat-plate one, and the cooling capacity reached the highest value at channel height of 0.005 mm (700 W for the irregular type and 650 W for the flat-plate one).

Fig. 12(d) indicates that the pressure drop in the irregular exchanger was 55.8% less than that in the flat-plat one, which was largely caused by the effect of the channel supporting guides. It should be noted that the pressure drop was calculated by using the K values derived from the CFD works.

5.2.2. Impact of the channel length

A large channel length leads to the increased heat and mass transfer rate, however, the power consumption of the cooler increases as well in order to overcome the flow resistance of the air travelling through the channels. Fig. 13(a) shows the variation trends of cooling capacity and COP versus the channel length, indicating that cooling capacity increased and the COP decreased when increasing the channel length. When the length varied from 0.2 m to 2 m, the changes in cooling capacity and COP were significant. When the length was beyond 2 m, the change tended to slow down. Therefore, it is not meaningful to consider channel length larger than 2 m for the cooler design. For the channel length from 1 m to 2 m, change in COP and cooling capacity became slower than that for the length from 0.2 m to 1 m. Therefore, the channel length of 1 m should be optimum choice for economic reason. This is because when the length was larger than 1 m the increased cooling capacity was in expense of more increased size and cost. However, in the case of that cooling capacity is the major concern rather than the size and cost, the channel length of 2 m is the best choice. In general, appropriate channel length for cooler design was considered to be between 1 m and 2 m, depending upon the users' preferences.

Fig. 13(b) shows variation of cooling effectiveness and outlet air temperature versus the channel length. The similar variation trends were found to the both exchangers as that in Fig. 13(a). These further proved that the appropriate channel length should be in the range 1 m–2 m. Fig. 13(c) shows that the pressure drop increased lineally with the channel length for the both exchangers. The average pressure drop of the irregular channel in the length range of 0.1 m–3 m was 56.2% lower than that of the flat-plat exchanger and the pressure drop difference between the two exchangers increased with the increase of channel length.

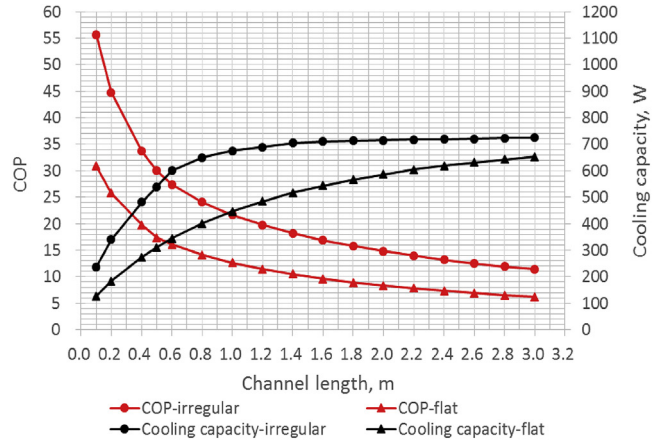

(a) Cooling capacity and COP

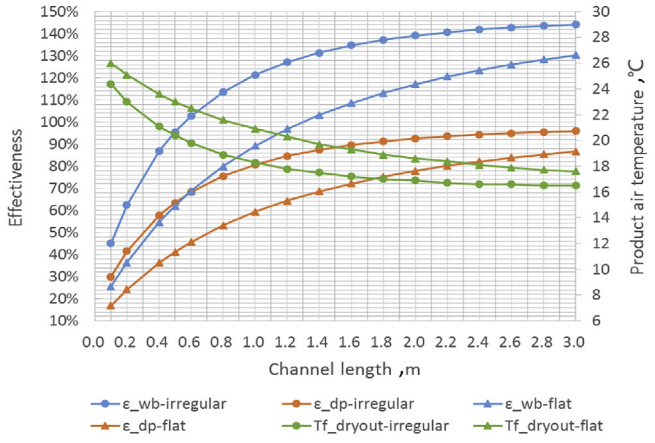

(b) Effectiveness and product air temperature

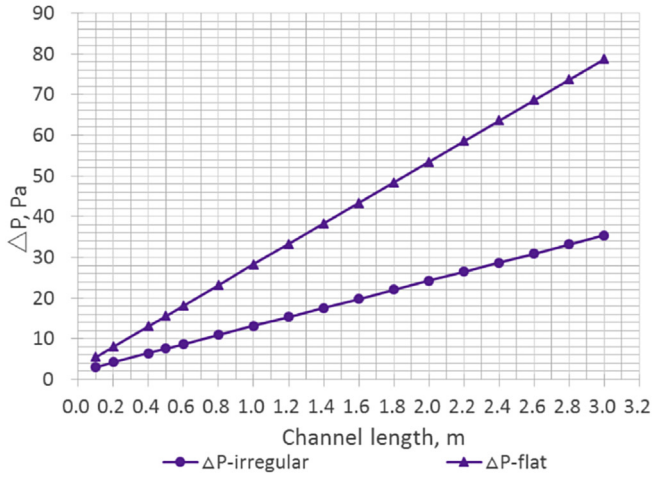

(c) Pressure drop

Fig. 13. Variation of performance with the channel length.

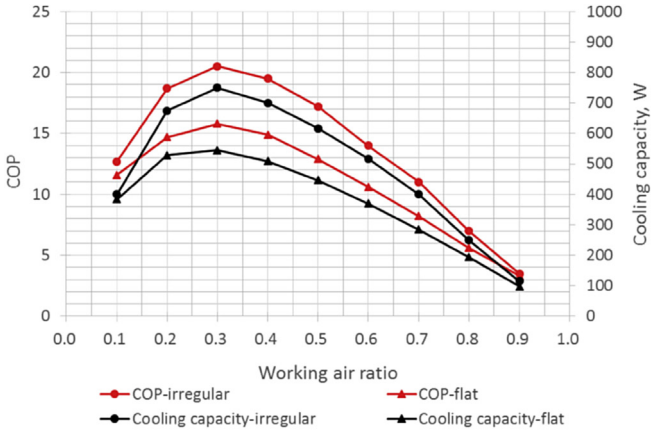

(a) Cooling capacity and COP

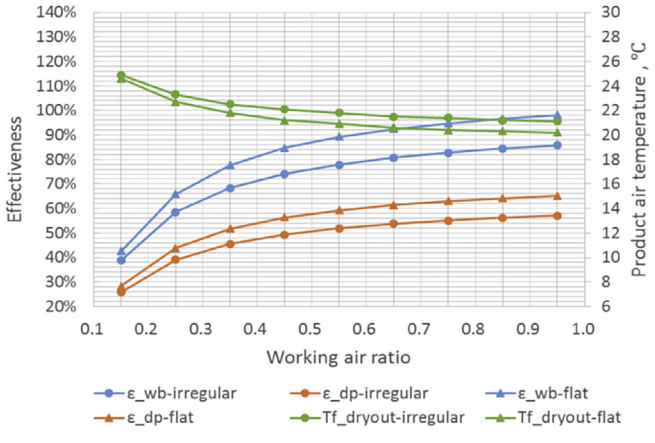

(b) Effectiveness and product air temperature

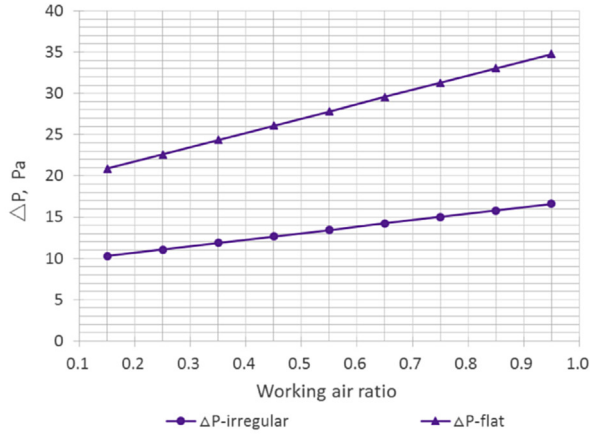

(c) Pressure drop

Fig. 14. Variation of performance with working air ratio.

5.3. Impact of the operational parameters

5.3.1. Impact of the working-to-intake air ratio

Working-to-intake air ratio is defined as the ratio of working air flow rate in the wet channel to the total intake air flow rate, which is the sum of the working air and product air. Higher working-to-intake air ratio could enhance the water evaporation in the wet channels, thus enhancing the cooling effectiveness of the heat and mass exchanger. However, this will also lead to the reduced product air flow rate and therefore reduced cooling capacity. Therefore, an optimum working-to-intake air ratio should be in existence to achieve the best balance between the cooling output and cooling efficiency. A dedicated investigation was carried out to optimize the working-to-intake air ratio and the results are shown in Fig. 14(a),

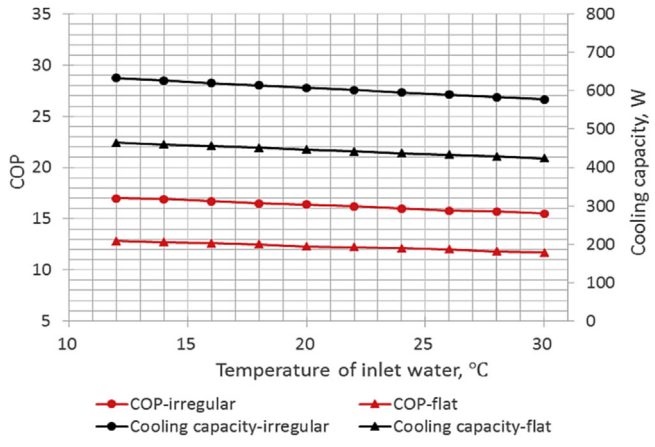

(a) Cooling capacity and COP

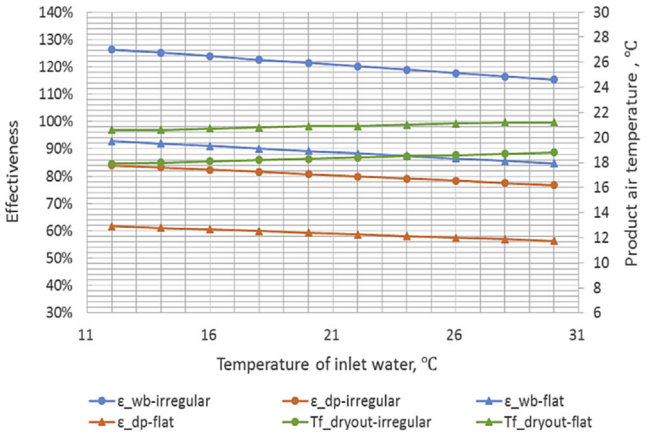

(b) Effectiveness and product air temperature

Fig. 15. Variation of performance with the temperature of inlet water.

(b) and (c).

It was found that the performance of both the irregular and flat-plate heat and mass exchangers showed similar trend of variation when the working-to-intake air ratio varied. For the both exchangers, Fig. 14(a) showed that the highest cooling capacities and COPs were at the working-to-intake air ratio of 0.3. Fig. 14(b) indicated that the cooling effectiveness increased with the increase of the working-to-intake air ratio; while the outlet product air temperature showed an opposite trend of the variation. However, these variations became slower when the working-to-intake air ratio was beyond 0.3. Fig. 14(c) showed that the pressure drop of the air through the channel increased linearly with the increase of the working-to-intake air ratio. Based on these findings, it was concluded that the optimum working-to-intake air ratio would be 0.3.

Compared to the flat-plate exchanger, the irregular type had higher COP, cooling capacity, dew-point and wet-bulb effectiveness, and lower outlet product air temperature. At the optimum working-to-intake air ratio of 0.3, their performance parameters were given as: (1) cooling capacity: 724.6 W vs. 545.2 W (32.9% higher); (2) COP: 20.5 vs. 15.8 (29.7% higher); (3) dew-point effectiveness: 68.7% vs. 51.7% (32.9% higher); and (4) wet-bulb effectiveness: 103.3% vs. 77.7% (32.9% higher).

5.3.2. *Impact of the water temperature*

During operation, water is circulated from a water container fitted beneath the wet channel outlet to the top of the wet channel by a pump. The water evaporates along the wet channel and extra water falls down to the water container. Water is continuously supplied to the water container to compensate the evaporated water. The temperature of the inlet water is therefore determined by the temperature and amounts of the water falling into the container and the supply water from the water source. The modelling work was carried out to investigate the effect of the inlet water temperature on the performance of the two types of heat and mass exchangers.

Fig. 15(a) shows the variation of the COP and cooling capacity versus the inlet water temperature and Fig. 15(b) shows the variation of the cooling effectiveness and outlet product air temperature versus the circulating water temperature. The flat curves indicate the effect of the circulating water temperature on the performance of the heat and mass exchangers was very minor.

Compared to the flat-plate exchanger, the irregular type showed a better performance in terms of the COP, cooling capacity, and cooling (dew-point and wet-bulb) effectiveness, which is similar to the previous case studies.

6. Conclusions

A novel irregular heat and mass exchanger with corrugated heat transfer surface and without the channel supporting guides has been presented. Combined CFD and finite-element based Newton-iteration numerical simulations indicated that the performance of the irregular heat and mass exchanger was superior to that of the existing flat-plate one, in terms of the cooling capacity, dew-point and wet-bulb effectiveness (around 32.9%–37% higher) at a range of geometrical and operational conditions. The COP of the dew point cooler with irregular exchanger was 29.7%–33.3% higher than that of the flat-plate one. By removing the need of channel support guides, the air flow pressure drop in the irregular channels was around 55.8%–56.2% lower than that in the flat-plate ones. The optimal design parameters of the novel irregular heat and mass exchanger are as follows: optimal intake air velocity is around 1 m/s, and optimal channel height and length of the both exchangers are 5 mm and 1–2 m respectively, while the appropriate working-to-intake air ratio is 0.3.

Owing to the enhanced energy and cooling performance, the novel irregular heat and mass exchanger will lead to reduced cost and size of the cooler at the same cooling output condition, and thus make it competitive to conventional mechanical vapour compression air conditioners.

Acknowledgement

The authors would acknowledge our sincere appreciation to the financial supports from the University of Hull, Engineering and Physical Sciences Research Council (EPSRC), Innovate UK and Ministry of Science and Technology of China (EP/M507830/1).

References

[1] Best R, Rivera W. A review of thermal cooling systems. Appl Therm Eng 2015;75:1162–75.
[2] Duan Z, Zhan C, Zhang X, Mustafa M, zhao X, Mustafa M, et al. Indirect evaporative cooling: past, present and future potentials. Renew Sustain Energy Rev 2012;16:6823–50.
[3] Boukhanouf R, Ibrahim HG, Alharbi A, Kanzari M. Investigation of an evaporative cooler for buildings in hot and dry climates. J Clean Energy Technol July 2014;2(3).
[4] Malli A, Seyf HR, Layeghi M, Sharifian S, Behravesh H. Investigating the performance of cellulosic evaporative cooling pads. Energy Convers Manag

2011;52:2598–603.
[5] Heidarinejad G, Bozorgmehr M, Delfani S, Esmaeelian J. Experimental investigation of two-stage indirect/direct evaporative cooling system in various climatic conditions. Build Environ 2009;44:2073–9.
[6] Zhan C, Duan Z, Zhao X. Comparative study of the performance of the M-cycle counter-flow and cross-flow heat exchangers for indirect evaporative cooling – paving the path toward sustainable cooling of buildings. Energy 2011;36:6790–805.
[7] Dean J, Herrmann L, Kozubal E, Geiger J. Dew point evaporative comfort cooling. Energy and water projects demonstration plan SI-0821, TP-7A40-56256-1. November 2012.
[8] Bruno F. On-site experimental testing of a novel dew point evaporative cooler. Energy Build 2011;43:3475–83.
[9] Kiran TR, Rajput SPS. Energy saving potential of a novel dew point evaporative air conditioning system for Indian buildings. Arch Appl Sci Res 2010;2(1):376–82.
[10] Lin J, Thu K, Bui T, Wang R, Ng KC, Chua KJ. Study on dew point evaporative cooling system with counter-flow configuration. Energy Convers Manag 2016;109:153–65.
[11] Elberling L. Laboratory evaluation of the Coolerado cooler-indirect evaporative cooling unit. Pacific Gas and Electric Company; 2006.
[12] VelascoGómez E, TejeroGonzá lez A, ReyMartıńez FJ. Experimental characterisation of an indirect evaporative cooling prototype in two operating modes. Appl Energy 2012;97(0):340–6.
[13] Riangvilaikul B, Kumar S. An experimental study of a novel dew point evaporative cooling system. Energy Build 2010;42:637–44.
[14] Tulsidasani T, Sawhney RL, Singh SP, Sodha MS. Recent research on an indirect evaporative cooler (IEC) part 1: optimization of the COP. Int J Energy Res 1997;21(12):1099–108.
[15] Riangvilaikul B, Kumar S. Numerical study of a novel dew point evaporative cooling system. Energy Build 2010;42:2241–50.
[16] Zhao X, Li JM, Riffat SB. Numerical study of a novel counter-flow heat and mass exchanger for dew point evaporative cooling. Appl Therm Eng 2008;28:1942–51.
[17] Zhan C, Zhao X. Numerical study of an M-cycle cross-flow heat exchanger for indirect evaporative cooling. Build Environ 2011;46:657–68.
[18] Cui X, Chua KJ, Yang WM. Numerical simulation of a novel energy efficient dew point evaporative air cooler. Appl Energy 2014;136:979–88.
[19] Cui X, Chua KJ, Islam MR, Yang WM. Fundamental formulation of a modified LMTD method to study indirect evaporative heat exchangers. Energy Convers Manag 2014;88:372–81.
[20] Sülar V, Öner E, Okur A. Roughness and frictional properties of cotton and polyster woven fabrics. Indian J Fibre Texile Res December 2013;38:349–56.
[21] Nag PK. Heat and mass transfer. 3th edition. Tata McGraw-Hill; 2011. p. 569.
[22] Incropera FP, Dewitt DP. Fundamentals of heat and mass transfer. sixth ed. , New York: John Wiley & Sons; 2007. p. 288–9.
[23] ASHRAE. American society of heating, refrigerating and air -conditioning engineers, vol. SI edition. ASHRAE handbook Fundamentals; 20094.18 [Chapter 4].
[24] White FM. Fluid mechanics. New York: McGraw-Hill; 1979. p. 353–6.
[25] Jradi M, Riffat S. Experimental and numerical investigation of a dew-point cooling system for thermal comfort in buildings. Appl Energy 2014;132:524–35.
[26] ASHRAE. ANSI/ASHRAE Standard 143-2000, Method of test for rating indirect evaporative coolers. American Society of Heating, Refrigerating and Air-Conditioning Engineers, Inc; 2000. GA 30329.
[27] Klein S, Nellis G. Mastering EES, F-Chart software. October 2014.
[28] Cellier FE, Kofman E. Continuous system simulation. Springer; 2006. p. 415–9.